

Characterization of excimer-laser-annealed polycrystalline silicon films grown by ultrahigh-vacuum chemical vapor deposition

Ying-Chia Chen, YewChung Sermon Wu, I-Chung Tung, Chi-Wei Chao, Ming-Shiann Feng, and Huang-Chung Chen

Citation: *Applied Physics Letters* **77**, 2521 (2000); doi: 10.1063/1.1318937

View online: <http://dx.doi.org/10.1063/1.1318937>

View Table of Contents: <http://scitation.aip.org/content/aip/journal/apl/77/16?ver=pdfcov>

Published by the [AIP Publishing](#)

Articles you may be interested in

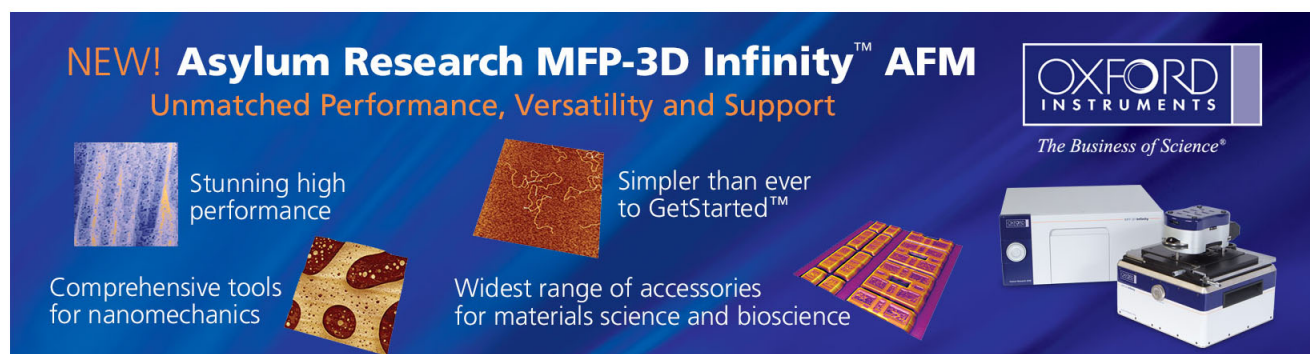
[Investigation of polycrystalline silicon grain structure with single wafer chemical vapor deposition technique](#)
J. Vac. Sci. Technol. A **19**, 1898 (2001); 10.1116/1.1355364

[Threshold voltage of excimer-laser-annealed polycrystalline silicon thin-film transistors](#)
Appl. Phys. Lett. **76**, 2442 (2000); 10.1063/1.126370

[Excimer laser annealing of amorphous and solid-phase-crystallized silicon films](#)
J. Appl. Phys. **86**, 5556 (1999); 10.1063/1.371560

[Characterization of excimer laser annealed polycrystalline Si_{1-x}Ge_x alloy thin films by x-ray diffraction and spectroscopic ellipsometry](#)
J. Appl. Phys. **83**, 174 (1998); 10.1063/1.366670

[Ex situ ellipsometry characterization of excimer laser annealed amorphous silicon thin films grown by low pressure chemical vapor deposition](#)
Appl. Phys. Lett. **71**, 359 (1997); 10.1063/1.119537

The advertisement features a dark blue background with white and orange text. At the top left, it reads 'NEW! Asylum Research MFP-3D Infinity™ AFM' in large white letters, followed by 'Unmatched Performance, Versatility and Support' in orange. To the right is the Oxford Instruments logo, which includes the text 'OXFORD INSTRUMENTS' and the tagline 'The Business of Science®'. Below the text are four images: a textured surface, a circular pattern, a grid of small squares, and the physical AFM instrument. Each image is accompanied by a short text description: 'Stunning high performance', 'Simpler than ever to GetStarted™', 'Comprehensive tools for nanomechanics', and 'Widest range of accessories for materials science and bioscience'.

Characterization of excimer-laser-annealed polycrystalline silicon films grown by ultrahigh-vacuum chemical vapor deposition

Ying-Chia Chen, YewChung Sermon Wu, I-Chung Tung, Chi-Wei Chao, Ming-Shiann Feng,^{a)} and Huang-Chung Chen^{b)}

Department of Materials Science and Engineering, National Chiao Tung University, Hsinchu 300, Taiwan, Republic of China

(Received 28 January 2000; accepted for publication 28 August 2000)

Polycrystalline silicon (poly-Si) films grown by ultrahigh-vacuum chemical vapor deposition (UHVCVD) system and then annealed by excimer laser at room temperature have been investigated for the applications in polycrystalline silicon thin-film transistors (poly-Si TFTs). The results showed that the grain size of the laser-annealed poly-Si film decreased with laser energy density when a lower laser energy density below 157.7 mJ/cm^2 was used. At about the threshold laser energy density ($\sim 134.5 \text{ mJ/cm}^2$), the finest grain structure could be obtained due to the partial melting in the top layer of the film. When the energy density of the excimer laser was larger than the threshold energy density, the large grain growth was initiated. The largest grain structure could be obtained at $\sim 184 \text{ mJ/cm}^2$, while its surface roughness was better than that of the nonannealed UHVCVD poly-Si films. The surface roughening was suggested to arise from the specific melt-regrowth process but not the rapid release of hydrogen or capillary wave mechanism derived from laser-annealed amorphous silicon. By use of the laser-annealed UHVCVD poly-Si films as the active layer, the fabricated poly-Si TFT exhibited a field-effect mobility of $138 \text{ cm}^2/\text{Vs}$, a subthreshold swing of 0.8 V/dec , a threshold voltage of 3.5 V , and an on/off current ratio of $\sim 10^6$.

© 2000 American Institute of Physics. [S0003-6951(00)03842-0]

Low-temperature polycrystalline silicon thin-film transistors (LT poly-Si TFTs) have attracted considerable attention for use in active matrix liquid crystal displays (AMLCDs) due to their better performance and the ability of integrating peripheral circuits on a low-cost glass substrate.^{1,2} The poly-Si films are usually fabricated by solid phase crystallization (SPC) of amorphous silicon (*a*-Si) films. In contrast to the SPC method, the excimer laser crystallization of *a*-Si, because it offers the lower thermal budget, shorter processing time, and high quality poly-Si films with higher crystallinity,³ seems to be the most attractive technique for fabricating LT poly-Si TFTs. The final quality of poly-Si TFTs is strongly dependent on poly-Si active layers (including grain structure and surface roughness).⁴⁻⁶ Asai *et al.*⁷ reported that the surface roughness would develop due to the differences in latent heat and thermal conductivity between polycrystalline and amorphous phase. McCulloch and Brotherton⁸ suggested that the rapid release of hydrogen from hydrogenated silicon films and optical interference effects in multiple shot crystallization will attribute to the surface roughness. Furthermore, Fork *et al.*⁹ proposed the capillary wave mechanism to describe the formation of surface roughness.

A 500-nm-thick wet oxide was grown on the top of p-type (100) silicon wafers. The silane-based polysilicon films with a thickness of $\sim 100 \text{ nm}$ were then deposited onto the wafers by a ultrahigh-vacuum chemical vapor deposition (UHVCVD) system at 550°C . The poly-Si films were irradiated by a KrF excimer laser (Lambda Physik LPX-200, λ

$\sim 248 \text{ nm}$) at room temperature with a N_2 flow rate of 50 sccm at a pressure of 800 mTorr . The laser beam spot, $1.8 \times 23.1 \text{ mm}^2$, was scanned with a 95% overlap from pulse to pulse, and its repetition rate was maintained at 20 Hz . An *n* and *k* analyzer was used to measure the optical properties of the thin films. The properties of the poly-Si films were examined by means of x-ray diffraction (XRD) and atomic force microscopy (AFM). For comparison, the silane-based *a*-Si films deposited by low-pressure chemical vapor deposition (LPCVD) system at 550°C were also used.

The TFTs were fabricated by defining the silicon islands as the active areas on the excimer-laser-annealed (ELA) UHVCVD poly-Si film. In turn, a 950-\AA -thick tetraethylorthosilicate/ O_2 oxide film was deposited by the plasma enhanced chemical vapor deposition system. Subsequently, a 3000-\AA -thick Si_2H_6 -based *a*-Si film was deposited at 470°C by the LPCVD system and lithographically patterned as the gates. The gate electrode and source/drain were doped by self-aligned phosphorus implantation at a dose of $5 \times 10^{15} \text{ ions/cm}^2$. Then dopant activation and crystallization of *a*-Si gate electrodes were performed at 600°C for 24 h in N_2 ambient. Finally, Al patterns for interconnections were formed after opening contact holes.

Figure 1 shows the reflectivity spectra of silicon films. Compared with the spectrum of the LPCVD *a*-Si film, the UHVCVD silicon films (with or without laser annealing) possesses two extra peaks at ~ 370 and $\sim 276 \text{ nm}$. These peaks are associated with the indirect transition (E_1) and direct transition (E_2) for crystalline silicon,¹⁰⁻¹³ and can be used to distinguish between amorphous and polycrystalline phases, meaning that the UHVCVD films are polycrystalline. The absorption coefficients ($= 4\pi k/\lambda$)^{12,14} at the wavelength of 248 nm are calculated to be $1.92 \times 10^6 \text{ cm}^{-1}$ and 1.78

^{a)} Author to whom correspondence should be addressed; electronic mail: msfeng@cc.nctu.edu.tw

^{b)} Department of Electronics Engineering and Institute of Electronics.

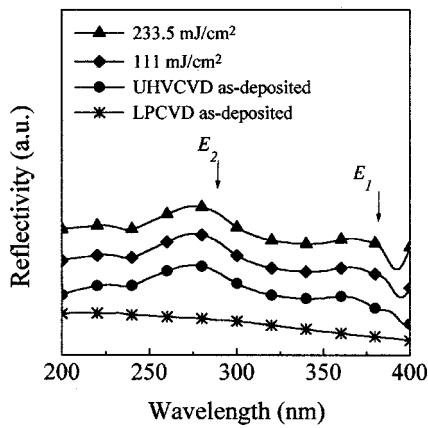


FIG. 1. The reflectivity spectra of as-deposited LPCVD *a*-Si film, as-deposited UHVCVD poly-Si film, and laser-annealed UHVCVD poly-Si films.

$\times 10^6 \text{ cm}^{-1}$ for LPCVD *a*-Si and UHVCVD as-deposited poly-Si, respectively. It exhibits that a 248 nm laser can also be used to anneal the as-deposited poly-Si.

Figure 2 shows the XRD Si (111) peak heights and surface roughness of the poly-Si films irradiated at different energy densities. The trend of peak heights is similar to that of surface roughness R_a . This trend is quite different from that of ELA *a*-Si. As is well recognized, for *a*-Si annealed by laser,^{15–18} the grain size increases gradually with increasing laser energy density until the energy reaches the threshold energy (E_{th}) for large grain growth to occur, at which the crystallinity increases dramatically. After the grain size reaches a peak value due to large grain growth, it decreases dramatically with further increases in laser energy density, since the homogeneous nucleation becomes more dominant in the crystallization process. In this ELA poly-Si film study, however, a minimum x-ray peak height (i.e., a minimum grain size) was found around E_{th} , as shown in Fig. 2. This is because some large grains may be only partially melted and the remaining unmelted fine crystallites serving as nucleation sites, which then gives a finest grain structure following the annealing. This will be further discussed later.

Figure 3 shows the AFM three-dimensional (3D) profiles of the UHVCVD as-deposited poly-Si films and the film irradiated with the laser energy of 184 mJ/cm². The as-deposited film shows surface with uniformly distributed bumps, which have been identified by transmission electron microscopy to be grains (~ 80 nm in size). On the other

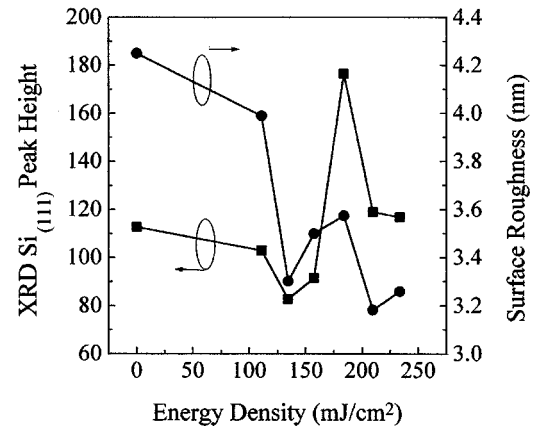


FIG. 2. The XRD Si (111) peak heights and surface roughness of ELA UHVCVD poly-Si films annealed at different laser energy densities.

hand, the bump surface of laser irradiated film accompanied with some concave areas, in which the bumps are ~ 200 nm in size. It is suggested that the regions around grain boundary melt by laser first and then extend into the grains. The large grains are anticipated to only be molten partially. (Compared with *a*-Si, as-deposited poly-Si film is harder to be melted.) Since the density of liquid silicon is higher than that of solid silicon and as-deposited poly-Si, the crystallization from the melt region would form the concave area, while the remaining unmelted small crystallites, serving as predetermined nuclei, would form the bumps surrounding each concave area. The concave area increases with laser density due to the increase of the melt region. By careful comparison between the AFM image [Fig. 3(b)] and the scanning electron microscopy (SEM) image (Fig. 4), a concave area does not represent a grain but contain several grains, which is different from the case for *a*-Si.¹⁹

Super-lateral-grain-growth (SLG) seems to not occur in the ELA UHVCVD poly-Si films. The largest grain morphology looks quite different from that of the ELA *a*-Si films, i.e., the large grains accompanied with very small grains. Besides, their largest grain sizes are even smaller than those of the as-deposited poly-Si film. Moreover, the origin of surface roughness for ELA UHVCVD poly-Si films shows quite different from that of the ELA *a*-Si films, such as the rapid release of hydrogen⁸ or the capillary wave mechanism.⁹ The surface roughness of the UHVCVD poly-Si films may arise from the melt-growth process as mentioned previously. The amorphous region around the

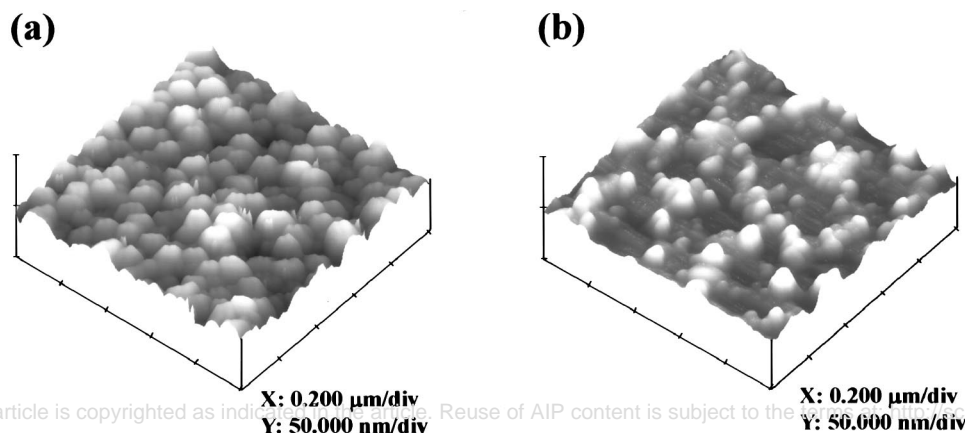


FIG. 3. The AFM 3D images of as-deposited UHVCVD silicon films (a) and those films irradiated with the laser energy density of 184 mJ/cm² (b).

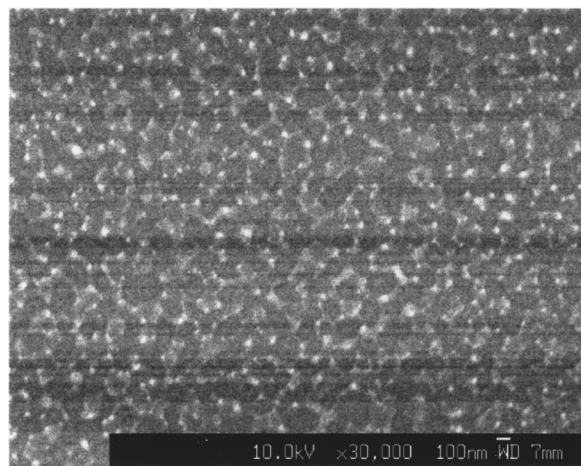


FIG. 4. The SEM images of as-deposited UHVCVD silicon film irradiated with a laser energy density of 184 mJ/cm^2 .

grain boundaries would melt first and extend into the grains, and the concave areas may form due to a sufficient melt region by melting several grains.

Figure 5 shows the I_d-V_g characteristics of ELA UHVCVD poly-Si film (with 184 mJ/cm^2 energy density). For comparison, the characteristics of the LPCVD a -Si film, the laser-annealed LPCVD poly-Si film, and the poly-Si film obtained from SPC (at 600°C for 24 h) of the LPCVD a -Si were also measured. The optimal laser-annealed UHVCVD poly-Si TFT shows a field-effect mobility of $138 \text{ cm}^2/\text{V s}$, a subthreshold swing of 0.8 V/dec , and a threshold voltage of 3.5 V , while the minimum current is as low as $1.95 \times 10^{-10} \text{ A}$ and the on/off current ratio is 10^6 for $V_d=5 \text{ V}$. This TFT device made from the laser-annealed UHVCVD poly-Si is good enough to satisfy the current application requirements.

Besides, both the as-deposited UHVCVD poly-Si and SPC LPCVD poly-Si give the mobility lower than $10 \text{ cm}^2/\text{V s}$ and on/off current ratio $\sim 10^5$ for $V_d=5 \text{ V}$. In contrast, the laser-annealed LPCVD poly-Si gives the much

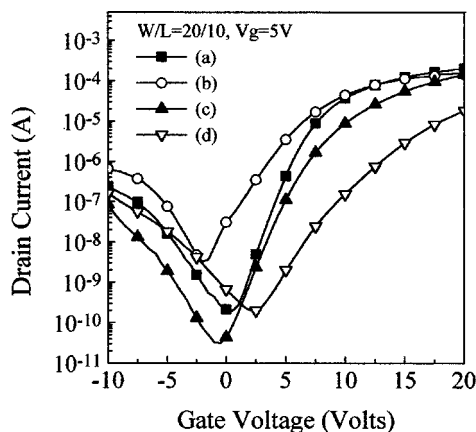


FIG. 5. The I_d-V_g characteristics of the fabricated LT poly-Si TFTs fabricated with various methods. (a) UHVCVD poly-Si+ELA (optimal condition: 184 mJ/cm^2), (b) UHVCVD poly-Si, (c) LPCVD a -Si+ELA (optimal condition: 195 mJ/cm^2), and (d) LPCVD a -Si+SPC (600°C , 24 h).

higher mobility $67 \text{ cm}^2/\text{V s}$, the subthreshold swing of 1.5 V/dec , and on/off current ratio larger than 10^6 for $V_d=5 \text{ V}$. This result clearly shows that electrical characteristics can be significantly improved by laser-annealing process. On the other hand, furnace annealing (at 600°C for 24 h for dopant activation) does not effectively improve electrical characteristics.

The ELA a -Si films are mostly crystallized via SLG for applications in poly-Si TFTs, thus simultaneously containing very large grains ($\geq 500 \text{ nm}$) and small grains ($\leq 50 \text{ nm}$).¹⁶ Therefore, the grain structure in the channel region of the TFT device may vary from device to device; some channels would contain a very large grain and a very small grain but some would contain several small grains. This structure variation may deteriorate the performance of AMLCDs. Fortunately, the ELA UHVCVD poly-Si films can alleviate this problem due to its uniform grain size ($\sim 100 \text{ nm}$), leading to a higher field effect mobility compared to the poly-Si TFTs fabricated by thermal annealing of a -Si ($\sim 10\text{--}80 \text{ cm}^2/\text{V s}$).^{20,21}

The authors would like to thank Professor Chun-Yen Chang for support on the UHVCVD work and Professor Huang-Chung Cheng for support on the excimer laser annealing work. This research was funded by the National Science Council (NSC) of the Republic of China under Grant No. NSC 89-2215-E-009-005. Technical support from the National Nano Device Laboratory of NSC and Semiconductor Research Center of National Chiao Tung University is also acknowledged.

¹T. Serikawa, S. Shirai, A. Okamoto, and S. Suyama, IEEE Trans. Electron Devices **36**, 1929 (1989).

²J.-I. Ohwada, M. Takabatake, Y. A. Ono, A. Mimura, K. Ono, and N. Konisji, IEEE Trans. Electron Devices **36**, 1923 (1989).

³T. Sameshima and S. Usui, J. Appl. Phys. **74**, 6592 (1993).

⁴K. Shimizu, O. Sugiura, and M. Matsumura, IEEE Trans. Electron Devices **40**, 112 (1993).

⁵M. Cao, S. Talwar, K. J. Kramer, T. W. Sigmon, and K. C. Saraswat, IEEE Trans. Electron Devices **43**, 561 (1996).

⁶F. Petinot, F. Plais, D. Mencaraglia, P. Legagneux, C. Reita, O. Huet, and D. Pribat, J. Non-Cryst. Solids **227–230**, 1207 (1998).

⁷I. Asai, N. Kato, M. Fuse, and T. Hamano, Jpn. J. Appl. Phys., Part 1 **32**, 474 (1993).

⁸D. J. McCulloch and S. D. Brotherton, Appl. Phys. Lett. **66**, 2060 (1995).

⁹D. K. Fork, G. B. Anderson, J. B. Boyce, R. I. Johnson, and P. Mei, Appl. Phys. Lett. **68**, 2138 (1996).

¹⁰G. Williams, D. Sands, R. M. Geatches, and K. J. Reeson, Appl. Phys. Lett. **69**, 1623 (1996).

¹¹C. H. Kuo, I. C. Hsieh, D. K. Schroder, G. N. Maracas, S. Chen, and T. W. Sigmon, Appl. Phys. Lett. **71**, 359 (1997).

¹²L. Ley, in *The Physics of Hydrogenated Amorphous Silicon II*, edited by J. D. Joannopoulos and G. Lucovsky (Springer, New York, 1984), p. 61.

¹³G. A. N. Connel, in *Amorphous Semiconductors*, edited by M. H. Brodsky (Springer, New York, 1979), p. 91.

¹⁴H. R. Philipp and E. A. Taft, Phys. Rev. **120**, 37 (1960).

¹⁵P. Baeri and E. Rimini, Mater. Chem. Phys. **46**, 169 (1996).

¹⁶M. Stehle, J. Non-Cryst. Solids **218**, 218 (1997).

¹⁷J. S. Im and H. J. Kim, Appl. Phys. Lett. **64**, 2303 (1994).

¹⁸G. K. Giust and T. W. Sigmon, Appl. Phys. Lett. **70**, 767 (1997).

¹⁹A. Marmorston, A. T. Voutsas, and R. Solanki, J. Appl. Phys. **82**, 4303 (1997).

²⁰T. Noguchi, A. J. Tang, and J. A. Tsai, IEEE Trans. Electron Devices **43**, 1454 (1996).

²¹L. Pichon, F. Raoult, K. Mourgues, K. Kis-Sion, T. Mohammed-Brahim, and O. Bonnaud, Thin Solid Films **296**, 133 (1997).